

*MOSTAFA A. NOUH\**, *NADIM M. ARAFA\**, *EHAB ABDEL-RAHMAN\**, \*\*

## STACK PARAMETERS EFFECT ON THE PERFORMANCE OF ANHARMONIC RESONATOR THERMOACOUSTIC HEAT ENGINE

A thermoacoustic heat engine (TAHE) converts heat into acoustic power with no moving parts. It exhibits several advantages over traditional engines, such as simple design, stable functionality, and environment-friendly working gas. In order to further improve the performance of TAHE, stack parameters need to be optimized. Stack's position, length and plate spacing are the three main parameters that have been investigated in this study. Stack's position dictates both the efficiency and the maximum produced acoustic power of the heat engine. Positioning the stack closer to the pressure anti-node might ensure high efficiency on the expense of the maximum produced acoustic power. It is noticed that the TAHE efficiency can further be improved by spacing the plates of the stack at a value of 2.4 of the thermal penetration depth,  $\delta_k$ . Changes in the stack length will not affect the efficiency much as long as the temperature gradient across the stack, as a ratio of the critical temperature gradient  $\Gamma$ , is more than 1. Upon interpreting the effect of these variations, attempts are made towards reaching the engine's most powerful operating point.

### 1. Introduction

Thermoacoustics is an emergent technology that uses the phenomenon of interaction of sound fields with solids to develop heat pumps or heat engines. A typical TAHE consists of a series of small parallel channels, referred to as a stack, sandwiched between a couple of heat exchangers and placed inside a resonator. The engine can be thermally driven by any source of heat, appealingly waste heat or concentrated solar power (Abdel-Rahman 2006). Upon heating the hot heat exchanger, induced acoustic wave can be converted to electricity thus introducing a novel environment-friendly power

---

\* *Department of Physics, The American University in Cairo, P.O. Box 74 New Cairo 11835, Cairo, Egypt; E-mail: mostafa.nouh@aucegypt.edu*

\*\* *The Yousef Jameel Science and Technology Research Center, The American University in Cairo, P.O. Box 74 New Cairo 11835, Cairo, Egypt*

converter. The operation of TAHE is based on acoustically excited parcels of working fluid to carry out a thermodynamic cycle with no piston. This can be achieved by exciting the working fluid in the presence of a temperature gradient. Basically, an acoustic wave travels up the temperature gradient while working gas parcels are in intimate thermal contact with the adjacent solid surfaces. While a parcel of gas is at its mean position and upon moving to higher temperatures, it is compressed, with a consequent rise in temperature. If the temperature rise is not sufficient to counteract the temperature increase in the adjacent surfaces (as the particle is displaced), heat is transferred to the gas during this compression phase. Conversely, heat is lost during the rarefaction. Energy will thus be added to the acoustic wave, with the gas executing an approximated Stirling cycle. In a standing wave thermoacoustic engine, the pressure and velocity fluctuations through the stack are such that heat is given to the oscillating gas at high pressure and removed at low pressure so as to satisfy Rayleigh's criterion (Swift 2001).

Rapid advancement in the field of thermoacoustics occurred only during the last three decades. Not having reached technical maturity, the energy conversion efficiency of thermoacoustic heat engines remains relatively lower than conventional counterparts (Paek 2006). However, the thermoacoustic technology is still advantageous due to the lack of moving parts in most of the devices conceived to date. Additionally, thermoacoustic devices utilize environmentally benign working fluids.

Numerous limitations affect the efficiency of TAHE, from inherent losses (heat transfer to and from the gas across the stack) to viscous losses incurred as the gas oscillates in the resonator. To enhance TAHE efficiency, higher power densities are needed, and hence a need to increase the acoustic pressure amplitudes. However, increasing the pressure amplitude should not be on the expense of generating nonlinear effects that will develop to shock formation and, in turn, to significant losses (Kinsler 1985). The need for high amplitudes with suppressed nonlinear effects calls for the use of anharmonic resonators.

The effect of using an anharmonic resonator of an elliptic shape on the quality of the resonator's performance is discussed in literature (Abdel-Rahman 2009). Fig. 1 highlights the motivation to investigate anharmonic resonators through a frequency response comparison between constant and variable area ducts. The trend suggests that more energy is expected to be devoted upon operating at the fundamental harmonic mode of the resonator, and consequently weaker performance at higher modes. Optimization of the resonator's geometry used in this work has been previously presented (Abdel-Rahman 2009). Yet, some of the critical design parameters remain in need of optimization to reach the maximum possible working efficiency that this design is capable of achieving. This work represents the discussion of the

stack-related parameters in an anharmonic resonator in order to reach optimum stack length, spacing and more importantly location.

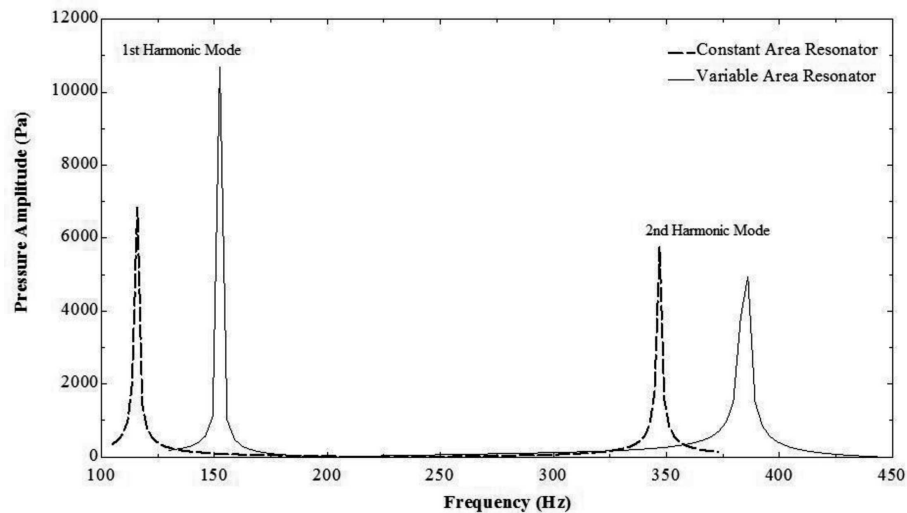


Fig. 1. Response of pressure amplitude to frequency variation for constant and variable area tubes of the same average diameter. The curve is drawn at a pressure of 1 bar using atmospheric air as the working fluid (Abdel-Rahman 2009)

## 2. Optimization of stack parameters in standing wave anharmonic TAHE

The computer code DeltaE is used to simulate and optimize the TAHE designed in this study. DeltaE solves the one-dimensional wave equation in gas or liquid, based on the low amplitude acoustic approximation in user defined geometries (Ward 2008). The procedure followed in this study is to study the effect of the stack location inside the resonator on both the efficiency and the acoustic power. For the optimized stack position, the effect of the stack's plate spacing on the efficiency has been studied. At the end, and for the optimized stack position and plates spacing, the effect of the stack length has been carried out.

### 2.1. Stack Positioning

The position of the stack within the device's resonator is one of the critical parameters that affect the design of TAHE. Positioning the stack depends on the design's main priority, and whether the design is to maximize the efficiency or the acoustic power. Stacks should typically be located whereas the magnitude of the gas velocity amplitude is relatively small to reduce the

viscous dissipation losses and therefore improve the efficiency (Swift 2001). Physically speaking, this implies situating the stack in a position where the magnitude of the local impedance  $Z$  is significantly large to satisfy equation (1), where  $\rho$  is the working gas density,  $a$  is the sound speed and  $A$  is the resonator's cross sectional area. On the other hand, the acoustic power generated in a standing wave engine is in continuous proportion with the imaginary portion of the product of pressure amplitude,  $p_1$  and volume velocity,  $U_1$ , according to equation (2) which implies having zero acoustic power if the stack is positioned at the pressure anti-node.

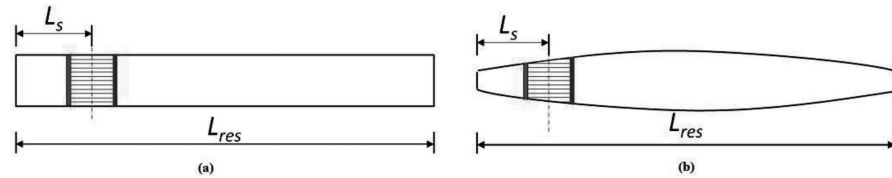


Fig. 2. Stack Center Position ( $L_s$ ) in (a) constant and (b) variable area resonators measured from the nearest pressure anti-node of  $\lambda/2$  standing wave engines

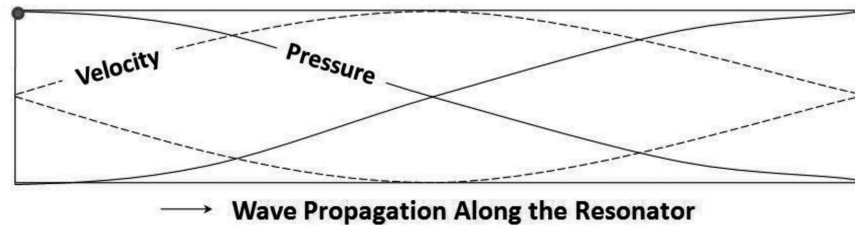


Fig. 3. Variation of pressure and velocity amplitudes along the resonator of a  $\lambda/2$  standing wave engine. The circle at the top left corner denotes the pressure anti-node nearest to the stack's location

Thus, a compromise between high power and high efficiency conditions is required. Given the fact that the stack position or location  $L_s$  is to be defined as the distance from midpoint of the stack to the nearest pressure anti-node in the resonator (Fig. 2), and that the normalized stack position  $L_{sn}$ , is the value of  $L_s$  expressed as a percentage of the wavelength  $\lambda$ , the typical  $L_{sn}$  suggested by literature is around one twentieth of the wavelength (Swift 2001). In other words, for a  $\lambda/2$  resonator, having a closed end and with a pressure anti-node at the left end (Fig. 3), the stack's center location,  $L_s$ , would be at 1/10 of the resonator's length.

$$|Z| > \frac{\rho a}{A} \quad (1)$$

$$\dot{E} \propto \text{Im}[p_1 U_1] \quad (2)$$

Pairing all the above information together, the optimal stack position is now known to be in the left half of the resonator, yet nearer to the end than to the resonator's center. Taking the typical  $\lambda/20$  ratio as a guideline, we can expect more generally the stack's position that will yield the optimum efficiency. This, however, does not necessarily imply the optimum stack's position for the anharmonic TAHE. In an attempt to reach the optimum stack location for this design, we used our modeling calculations to vary the stack position along the tube and detect for each case the power and efficiency variations of the device. The efficiency  $\eta$  in this study is defined by:

$$\eta = \frac{\dot{E}_{st}}{\dot{H}_{H,HX}} \% \quad (3)$$

where  $\dot{E}_{st}$  is the generated acoustic power along the stack and  $\dot{H}_{H,HX}$  is the heat input at the hot heat exchanger. Neglecting viscous losses  $\dot{E}_{st}$  can be estimated using eq. (4) (Symko 2004).

$$\dot{E}_{st} = \frac{1}{4} \prod \delta_k \Delta x \frac{T_m \beta^2 \omega}{\rho_m c_p} p_1^2 (\Gamma - 1) \quad (4)$$

where  $\Pi$  is the total effective circumference around the stack perpendicular to the heat flow direction,  $\delta_k$  is the thermal penetration depth,  $\Delta x$  is the stack's length in the acoustic wave propagation direction,  $T_m$  is the gas mean temperature across the stack,  $\beta$  is the gas expansion coefficient,  $\omega$  is the angular frequency,  $\rho_m$  is the mean density,  $c_p$  is the isobaric heat capacity and  $\Gamma$  represents the temperature gradient across the stack as a ratio of the critical temperature gradient. Eq.(4) will only yield a positive value when  $\Gamma$  exceeds unity, in which case the power will be generated in the stack instead of being consumed. In other words, the device will perform as a heat engine rather than a refrigerator. The efficiency can further be evaluated as a percentage of Carnot's efficiency,  $\eta_c$ . Noting, Carnot efficiency is the thermal efficiency of a Carnot heat engine cycle working on the same temperature difference. Given that  $T_H$  and  $T_A$  are the hot and ambient temperatures of the stack ends in degree Kelvin,  $\eta_c$  would then be (Boles 2002):

$$\eta_c = \frac{T_H - T_A}{T_H} \% \quad (5)$$

In this case, TAHE efficiency can be expressed in terms of  $\eta_c$  to give a relative normalized efficiency  $\eta_n$ :

$$\eta_n = \frac{\eta}{\eta_c} \% \quad (6)$$

Efficiency can also be expressed directly as a function of the critical temperature gradient and the temperature span across the stack (Symko 2004) given that  $\Delta T$  is the difference between  $T_H$  and  $T_A$ :

$$\eta = \left( \frac{\Delta T}{T_m} \right) \frac{1}{\Gamma} \quad (7)$$

Variation of the stack's location has been used to monitor several aspects that can lead to better interpretation of the behavior of the stack's position in the resonator. At a frequency in the order of 400 Hz, mean pressure of 10 bars and a temperature span of about 340 K across the stack, a parallel plate stack configuration was used to model the anharmonic TAHE. Helium was used as a working gas, being the most thermally conductive inert gas and the one possessing the highest sound velocity. Seven different stack positions are being used throughout the study. The locations vary from 6 to about 14% of the wavelength. In order to ease the illustration of results in the coming sections, these seven locations are mentioned in Table (1) and denoted corresponding alphabetical letter symbols.

Table 1.  
Different stack locations used in this study expressed in terms of the normalized stack position  $L_{sn}$  with the corresponding letter symbols

$L_{sn}$ (%)						
A	B	C	D	E	F	G
6.32	6.79	7.88	10.59	11.64	13.29	14.04

The first phase of optimization includes calculating the maximum acoustic power being generated at each of the different stack positions from A to G. For a design that's power oriented, that is a design aiming at maximizing the acoustic power (even if it is at the expense of the efficiency), this calculation would be of great help. Fig. 4 shows the maximum acoustic power that can be theoretically achieved using the different stack locations along with the corresponding device efficiency. The pattern shows a good agreement with our previous arguments. Whilst greater efficiencies require the stack to be closer to the pressure anti-node, higher power outputs could not be achieved except at further distances from that anti-node. It's obvious however that there is an optimum point for producing the highest acoustic power that is around location D. For example, among our seven comparison locations, the requirement for a power output of beyond 2.2 kW would require the stack to be positioned at D. The challenge still remains in solving for the best location to achieve lower power intensities. An example of this would be that at a required design output of 1 kW, there are apparently several possible options.

Any stack position starting from C up to G, and perhaps beyond that point which is beyond the domain of the calculations, is capable of producing an acoustic power of 1 kW. To take another insight into the stack location behavior that may help in taking such a decision, both the power and the corresponding efficiency were plotted for different thermal inputs to the hot heat exchanger independently for stack positions C, D, E, F and G (Fig. 5).

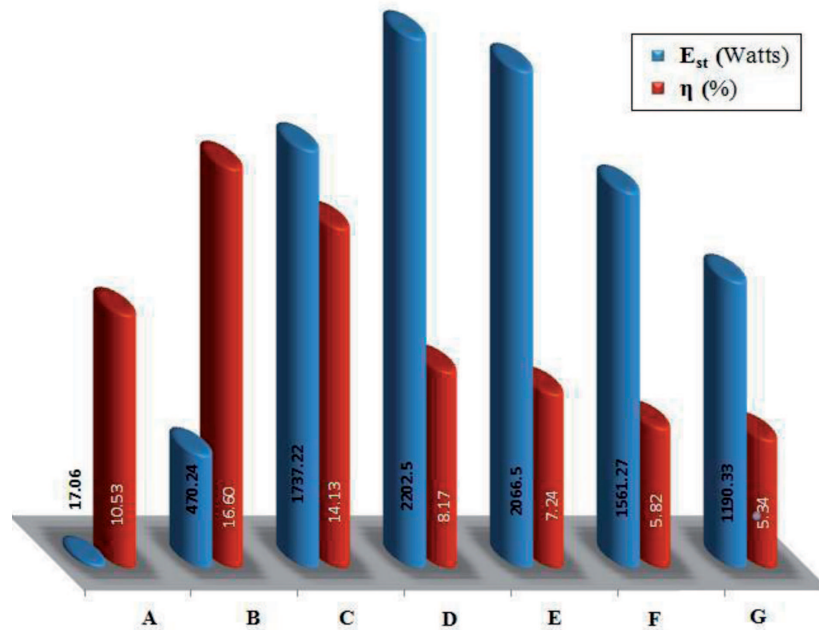


Fig. 4. Maximum achievable acoustic power generation in the stack at stack locations A – G and the corresponding efficiency at each maximum power point

The two red circle labels in each of the plots of Fig. 5 highlight the point of maximum efficiency and the point of maximum power achievable. An obvious overlap exists between these plots showing that, at a certain demanded power output, several possibilities for the stack location are available that can satisfy this desired design power. Using such curves, one can match the required power from the system with the most efficient choice of placing the stack. Discussing our previous example of the 1 kW power output, we can achieve that using stack position C with 14.56% efficiency, stack position D at 9.21%, stack position E at 8.25%, stack position F at 6.56% and finally stack position G at 5.79%. For this example, position C is the optimum stack location, but as we desire higher powers, the capability of the smaller stack positions to fulfill that requirement diminishes. The maximum powers that can be achieved at stack locations further away from the pressure anti-node

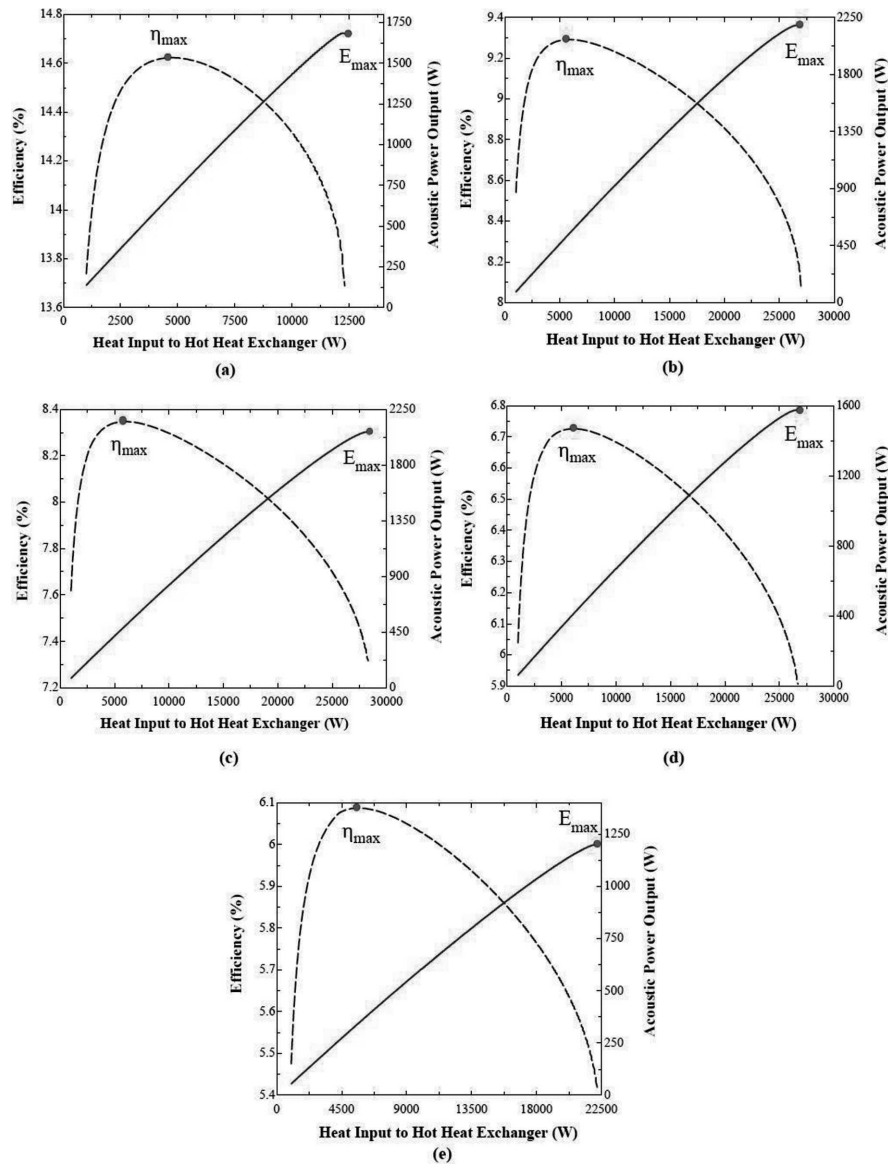


Fig. 5. Stack efficiency and generated acoustic power against heat input at stack positions (a) C, (b) D, (c) E, (d) F, (e) G

are higher which makes these positions advantageous at applications where higher powers are needed.

## 2.2. Plate spacing

One of the most critical parameters of the stack of any thermoacoustic device is its hydraulic radius  $r_h$  which is the ratio of the stack's cross-sectional



area to the perimeter of the gas channel. In parallel plate stacks, the hydraulic ratio is equivalent to half the spacing between two parallel plates,  $y_o$  (Tijani 2002). This is consecutively a very sensitive parameter that affects the stack's performance. The plate spacing determines the degree of thermal interaction between the gas flowing over the plates and the stack boundary, which is the kind of interaction we need to optimize to obtain maximum heat transfer. To evaluate this physically, we need to define another quantity which is the thermal penetration depth,  $\delta_k$ .

$$\delta_k = \sqrt{\frac{2k}{\rho c_p \omega}} \tag{8}$$

where  $k$  is the working gas thermal conductivity.  $\delta_k$  is where the gas particle in its stream of flow thermally interact with the surface enclosing it. At the same time, the viscous penetration depth,  $\delta_v$  is a region where the gas particle experiences viscous losses that obstacle its movement.

$$\delta_v = \sqrt{\frac{2\mu}{\rho \omega}} \tag{9}$$

where  $\mu$  is the working gas dynamic viscosity. Along with the thickness of the single plate  $2l$ ,  $y_o$  also controls the degree of porosity of the stack, or in other words the portion of the channels through which the working gas is expected to flow through as compared to the solid area of the stack. The porosity ratio, also denoted the blockage ratio,  $B$ , is expressed as:

$$B = \frac{y_o}{y_o + l} \tag{10}$$

A certain limit has to be imposed on the value of  $y_o$  such that we can obtain our desired heat transfer whilst minimizing viscous losses that can negatively affect the performance. In order not to alter the acoustic field, twice  $y_o$  is preferably selected to be in the range of 2-4  $\delta_k$  (Wheatley 1985). Optimization within this range is yet still possible. Fig. 6 highlights the efficiency's varying behavior against the change in the normalized plate spacing which is the ratio  $y_o/\delta_k$ . With the frequency, temperature span and mean gas pressure held the same as mentioned in the previous section. Fig. 6 examines the reaction of slightly changing the plate spacing at stack position C at a heat input to the hot heat exchanger of 2000 W. From Fig. 5 (a) the expected efficiency is 14.3%, which can be raised further to values as high as 14.8% (Fig. 6) by slight optimization of the plate spacing. The normalized plate spacing at the point of best efficiency is within the order of 1.2, which makes the plate spacing  $2y_o$  about 2.4 of the thermal penetration depth,  $\delta_k$ .

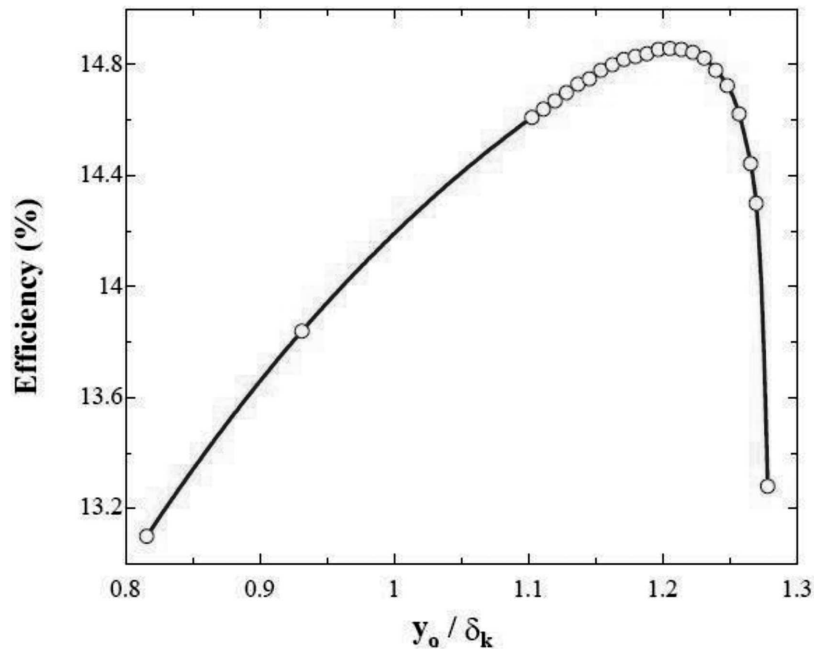


Fig. 6. Efficiency against normalized spacing of the stack plates at a constant thermal input of 2000 W to the hot heat exchanger, a frequency of 398 Hz, temperature difference of 340 K and mean helium pressure of 10 bars

### 2.3. Stack length

The term stack length is conventionally used to define the length of the stack in the acoustic field propagation direction and is denoted  $\Delta x$  in this work (Fig. 7). The stack length was previously mentioned in Eq. (4). As noted in this equation, the amount of heat pumped by the stack is directly proportional to the stack length. There is, however, another perspective that puts a ceiling to the growth of  $\Delta x$ . The term  $\Gamma$  which represents the temperature gradient across the stack as a ratio of the critical temperature gradient is governed by (Tijani 2002):

$$\Gamma = \frac{\Delta T_m}{T_m(\gamma - 1)B\Delta x k} \tan(k_n L_s) \quad (11)$$

where  $\gamma$  is the ratio of isobaric to isochoric specific heats of the working gas,  $k_n$  is the wave number defined as  $2\pi/\lambda$ . As discussed earlier,  $\Gamma$  must exceed unity for our design to work as a heat engine or a prime mover, i.e. generate acoustic power across the stack length rather than consume any. For this to occur, the stack's length  $\Delta x$  should now be carefully comprised to achieve maximum achievable power (Eq. 4) and still satisfy the heat engine condition (Eq. 11). Fig. 8 shows the efficiency variation at a constant heat input, which simply can be taken as an indicator of power variation, against

slight variation of the stack's length. The same comparison parameters are kept as in Fig. 6 (i.e. 2000 W of heat input and stack location C). The sudden drop after the dashed vertical red line indicates that the design is going beyond the power generation limit and is shortly starting to witness a  $\Gamma$  less than 1, at which case the resonator will function as a thermoacoustic cooler. This consequently acts as the maximum limit for further increase of the stack's length in the design.

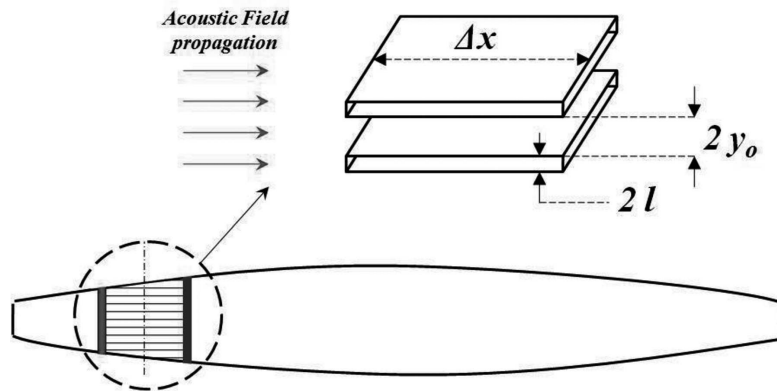


Fig. 7. Geometrical parameters of a parallel plate stack

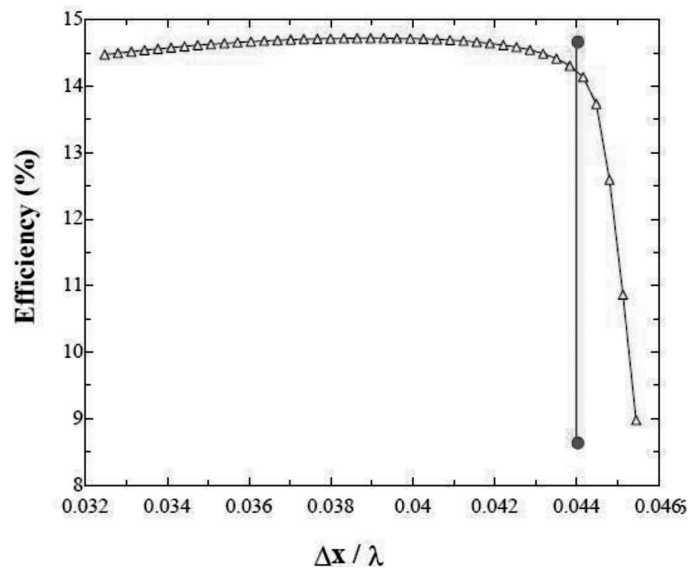


Fig. 8. Efficiency against the stack length as a ratio of the wavelength at a constant thermal input of 2000 W to the hot heat exchanger, a frequency of 398 Hz, temperature difference of 340 K and mean helium pressure of 10 bars

### 3. Summary and Conclusions

The optimal design for a stack filled with parallel plates in a standing-wave anharmonic thermoacoustic heat engine was studied. The relationship between efficiency and stack's position, length and the plate spacing is investigated in the novel resonator shape. Whilst greater efficiencies require the stack to be closer to the pressure anti-node, higher power outputs could not be achieved except at further distances from that anti-node. Higher efficiency can be achieved at normalized plate spacing within the order of 1.2 which makes the plate spacing  $2y_o$  about 2.4 of the thermal penetration depth,  $\delta_k$ . The design tolerates variations in the stack length as long as it is less than 0.042 of the wavelength. This study contributes to further improvement in TAHE development.

### Acknowledgment

This research is supported by KAUST (AUC-KAUST Integrated Desert Building Technologies project).

Manuscript received by Editorial Board, January 09, 2013;  
final version, October 02, 2013.

### REFERENCES

- [1] Ehab Abdel-Rahman, Mahmoud Hammam, Mahmoud Salah, and Samy Abdel-Mordy: Design, development and testing a solar concentrator for thermoacoustic cooling applications. *International journal of pure and applied physics (IJPAP)*, Vol. 2, No. 1, 99-109 (2006).
- [2] Mostafa A. Nouh, Nadim M. Arafa, Krister Larsson, Ehab Abdel-Rahman: Design study of an anharmonic resonator standing wave thermoacoustic heat engine. *Proceedings of the 16<sup>th</sup> International Congress on Sound and Vibration (2009)*.
- [3] Swift G.W.: *Thermoacoustics: A unifying perspective for some engines and refrigerators*. The Acoustical Society of America, Melville, NY (2002).
- [4] Yunus A. Cengel, Michael A. Boles: *Thermodynamics: An Engineering Approach*. McGraw Hill, NY (2002).
- [5] Swift G.W.: Analysis and performance of a large thermoacoustic engine. *J. Acoust. Soc. Am.* 92: 1551-1563 (1992).
- [6] Swift G.W. Thermoacoustic engines. *J. Acoust. Soc. Am.*; 84:1145-1179 (1988).
- [7] Swift G.W. Thermoacoustic engines and refrigerators. *Encyclopedia Appl. Phys.* 21: 245-264 (1997).
- [8] Hadi Babaei, Kamran Siddiqui. Design and optimization of thermoacoustic devices. *Energy Conversion and Management* 49: 3585-3598 (2008).
- [9] Symko O.G., Abdel-Rahman E., KWON Y.S., Emmi M., Behunin R.: Design and development of high-frequency thermoacoustic engines for thermal management in microelectronics. *Microelectronics Journal* 35: 185-191 (2004).
- [10] Tijani M.E.H., Zeegers J.C.H., De Waele A.T.A.M.: Design of thermoacoustic refrigerators. *Cryogenics* 42: 49-57 (2002).

- [11] Lawrence E. Kinsler, Austin R. Frey, Alan B. Coppins, James V. Sanders: Fundamentals of acoustics, third edition. John Wiley & Sons NY (1985).
- [12] Wheatley J.C., Hofler T., Swift G.W., Migliori A.: Understanding some simple phenomena in thermoacoustics with applications to acoustical heat engines. Am. J. Phys. 53: 147-162 (1985).
- [13] Ward B., Clark J., and Swift G.W.: Design environment for low-amplitude thermoacoustic energy conversion, DELTAEC version 6.2: Users guide. Los Alamos national laboratory (2008).

### **Wpływ parametrów stosu na osiągi anaharmonicznego rezonatora termoakustycznej maszyny cieplnej**

#### S t r e s z c z e n i e

Termoakustyczna maszyna cieplna (TAHE) przekształca ciepło w energię akustyczną bez użycia części ruchomych. W porównaniu z maszynami tradycyjnymi ma ona szereg zalet, takich jak prosta konstrukcja, stabilność działania oraz wykorzystanie gazów przyjaznych dla środowiska. W celu dalszej poprawy osiągnięć maszyny TAHE należy zoptymalizować parametry stosu (zespołu wąskich kanałów między płytami wymiennika ciepła). Trzema głównymi parametrami analizowanymi w przedstawionej pracy są pozycja stosu, długość i odstęp między płytami. Pozycja stosu decyduje zarówno o sprawności jak maksymalnej mocy akustycznej wytwarzanej przez maszynę cieplną. Umieszczenie stosu bliżej strzałki fali stojącej może zapewnić większą sprawność kosztem maksymalnej wytwarzanej mocy akustycznej. Stwierdzono, że dalsza poprawa sprawności maszyny TAHE może być osiągnięta gdy zastosuje się odstęp płyt stosu równy 2,4 cieplnej głębokości wnikania,  $\delta_k$ . Zmiany długości stosu nie mają wielkiego wpływu na sprawność tak długo, jak stosunek krytycznego gradientu cieplnego  $\Gamma$  jest większy od 1. Na podstawie interpretacji efektów tych zmian podjęto wysiłki dla uzyskania najlepszych osiągnięć maszyny.